JOURNAL OF CATALYSIS 50, 109–114 (1977)

Active Sites in Zeolites

Part 7. Isopropanol Dehydrogenation over Alkali Cation-Exchanged X and Y Zeolites

PETER A. JACOBS AND JAN B. UYTTERHOEVEN

Centrum voor Oppervlaktescheikunde en Colloïdale Scheikunde, Katholieke Universiteit Leuven, De Croylaan 42, B-3030 Heverlee, Belgium

Received March 1, 1977

The dehydrogenation of isopropanol has been followed in a flow reactor in the differential mode over alkali cation- and lanthanum-exchanged X and Y zeolites with controlled amounts of iron impurities. Two maxima are observed in the rate of acetone formation. A linear correlation was found between the dehydrogenation rate and the residual iron content of the catalysts. The reaction rate was not susceptible to pyridine addition, but could be suppressed upon addition of acetonitrile. Similarities between H_2–D_2 exchange and acetone formation have enabled a detailed reaction mechanism to be advanced, with the associative desorption of hydrogen determining the rate.

INTRODUCTION

Dehydrogenation of primary and secondary alcohols into aldehydes and ketones, respectively, is one of the major routes of synthesis of these products (*1*).

The mechanism of alcohol dehydrogenation over the conventional dehydrogenation catalysts has hardly been investigated. Over hydroxyapatite catalysts (*2*) dehydrogenation of alcohols was pictured as occurring via a concerted mechanism over an acid–base pair of sites. The dehydrogenation of 2-propanol over alkali cation-exchanged zeolites X and Y was investigated in the high-temperature region (above 450°C) (*3*). The dehydrogenation/dehydration selectivity was found to be dependent on the nature of the alkali cation (*3*).

In Part 6 of this series (*4*), the low-temperature dehydration of alcohol was reported over alkali cation-exchanged zeolites. Under these conditions, the dehydration was found to occur via an E_1 elimination reaction over hydroxyl groups.

In this work, the dehydrogenation of isopropanol is investigated over alkali cation and rare earth-exchanged faujasites in the low-temperature region. A mechanism is proposed as well as a model for the active sites.

EXPERIMENTAL

Materials. The parent Linde NaX and NaY zeolites used in Part 6 of this series (*4*) contained, as main impurities, 1150 and 913 ppm of iron, respectively, as determined by neutron-activation analysis. Fully exchanged LiY and KY zeolites were prepared by conventional ion exchange. The parent NaY sample has been purified by treatment with ultrapure NaCl solution, or with sodium acetate solution, or with dithionite solution as described previously (*5*). The iron content of each sample was again determined by neutron-activation analysis.

ISSN 0021-9517

La^{3+} ions were exchanged into the NaX and NaY zeolites using a diluted $La(NO_3)_3$ solution of 1.5 mmol dm^{-3} and a solid to liquid ratio of 0.5 g $liter^{-1}$. These precautions were taken to minimize cation hydrolysis during the ion exchange. In this way, zeolites with the following anhydrous unit cell compositions were obtained:

LaX: $(La)_{21.3}(Na)_{21.3}(AlO_2)_{85}(SiO_2)_{107}$,

LaY: $(La)_{12.8}(Na)_{16.5}(AlO_2)_{55}(SiO_2)_{137}$.

The numbers after the catalyst in the sample notation refer to the degassing temperature in degrees centigrade.

The reactants used, viz., isopropanol, propanol, ethanol, and butanol, were of analytical grade from Merck. Pyridine and acetonitrile were of "Uvasol" purity and also were from Merck.

Methods. The previously described (*4*) semiautomatic continuous-flow reactor was used in the differential mode and was operated at atmospheric pressure. The standard reaction conditions used were: flow rate, 60 ml min^{-1}; isopropanol pressure, 28 Torr, diluted with helium. It was verified that diffusion-free reaction rates could be obtained in this way (*4*).

Pretreatment of the catalysts was carried out *in situ* using dry and 99.99% pure helium, hydrogen, or oxygen from Air Liquide.

TABLE 1

Dehydrogenation of Isopropanol over NaY-400 Using Different Degassing Atmospheres

Pretreatment atmosphere at 400°C	Rate of acetone formation at 120°C ($mol\ g^{-1}\ s^{-1} \times 10^9$)
Helium	1.45
Hydrogen	2.09
Oxygen	1.25
Hydrogen + oxygen	1.30
Oxygen + hydrogen	2.15

RESULTS

At the low conversions used, no appreciable deactivation with respect to acetone formation occurred. Over a NaY-400 catalyst at 120°C the selectivity for dehydrogenation was 38.5%, and hydrogen was formed as a reaction product. The other products were propylene and diisopropyl ether, resulting from a dehydration reaction.

Variation of Dehydrogenation with the Degassing Atmosphere

It was found that the rate of isopropanol dehydrogenation was susceptible to the atmosphere in which the catalyst was degassed before reaction. Table 1 shows that the most active dehydrogenation catalyst was obtained after hydrogen pretreatment. Upon oxygen treatment the rate slowed down but regained its initial value upon subsequent hydrogen treatment. This peculiar behavior was also observed for the hydrogen–deuterium equilibration rate after the same treatments (*5*). The rate of dehydration was not affected after the treatments mentioned in Table 1.

Influence of the Degassing Temperature

Figure 1 illustrates the variations of the rate of acetone formation upon degassing of the NaY catalyst. A two-maxima pattern is observed for the reaction rates. The first maximum is around 400°C, the second one around 640°C. The true activation energy remains constant up to activation temperatures of 500°C and then gradually decreases. Here again, there exists a remarkable similarity between the behavior of NaY during isopropanol dehydrogenation and the high-temperature hydrogen–deuterium equilibration (*5*).

The same two-maxima pattern for H_2–D_2 exchange over NaY was also observed over LaY and LaX zeolites (*5*). In order

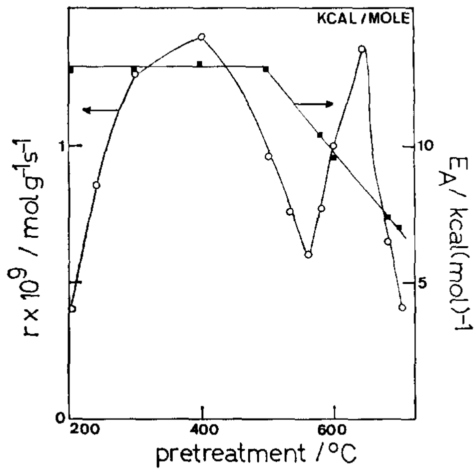

FIG. 1. Change of the dehydrogenation rate of isopropanol (r) at 120°C and of the apparent activation energy (E_A) with the degassing temperature of NaY.

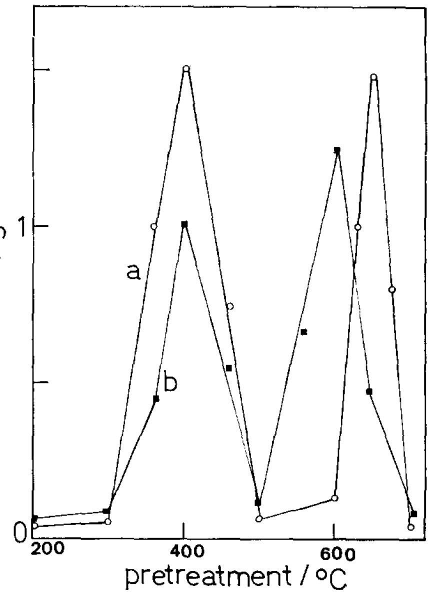

FIG. 2. Change of the dehydrogenation rate of isopropanol (r) at 120°C with the degassing temperature over LaX (a) and LaY (b).

to extend the similarity between the two types of reactions, the rate of acetone formation at increasing outgassing temperatures is shown in Fig. 2. For both catalysts two maxima located in the same temperature region are observed. The absolute values of the dehydrogenation rates, therefore, are strongly dependent on the activation temperature, but much less on the nature of the major charge-compensating cation: The rates of acetone formation over NaY (Fig. 1) and over LaX or LaY (Fig. 2), activated at the same temperature, hardly differ.

Influence of the Nature of the Alkali Cation

In order to verify the high-temperature results of Yashima *et al.* (*3*) at low reaction temperatures, the dehydrogenation of isopropanol over alkali cation-exchanged Y zeolites was determined. The change in the rate of acetone formation with the inverse radius of the cation is shown in Fig. 3 (curve a). No linear relationship is observed. Yashima *et al.* (*3*) found that, at reaction temperatures above 400°C, the rate of acetone formation increased with the size of the alkali cation. The rates of olefin and ether formation steadily decrease with the size of the alkali cation (*4*). When the rate of acetone formation is plotted against the residual iron content of the zeolites (Fig. 3, curve b), a linear relationship with a positive slope is observed.

In order to generalize the relation between the rate of acetone formation and

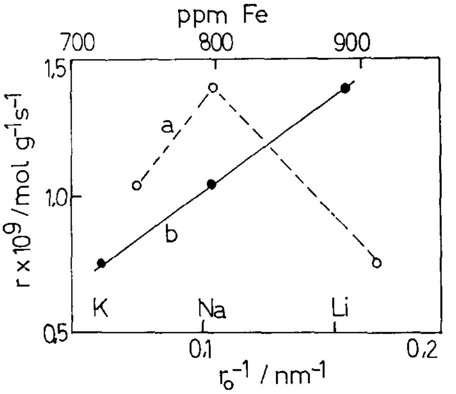

FIG. 3. Influence of the inverse radius (r_o^{-1}) of the cations of alkali cation-exchanged zeolites (a) degassed at 400°C and influence of the residual iron content of these catalysts (b) on the rate of isopropanol dehydrogenation at 120°C.

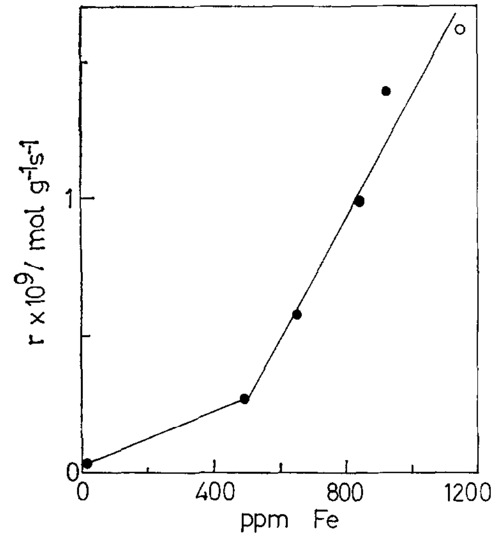

FIG. 4. Dependence of the rate of isopropanol dehydration at 120°C on the residual iron content of NaY-400 (●) and NaX-400 (○) samples.

the residual iron content of the zeolites, purified samples differing in their residual iron content were prepared (*5*) and tested for the rate of acetone formation. Figure 4 shows that there exists a positive relationship: The higher the residual iron content of the zeolite, the more pronounced is the dehydrogenation of isopropanol.

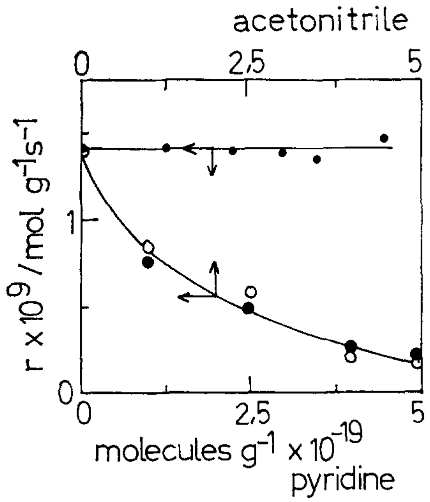

FIG. 5. Poisoning of the dehydrogenation of isopropanol at 120°C over NaY with pyridine and acetonitrile: (●) NaY-400; (○) NaY-650.

Poisoning

Figure 5 shows that the formation of acetone from isopropanol is not susceptible to poisoning with pyridine, in contrast to the dehydration rate (*4*). The same figure shows that the dehydrogenation activity of NaY can almost be eliminated after addition of 5 × 10^{19} molecules of acetonitrile at 400°C per gram of catalyst. This corresponds very closely to the amount of poison needed for suppression of H_2–D_2 equilibration activity (*5*).

Influence of the Alcohol Structure

Kibby and Hall (*2*) reported that, over hydroxyapatite catalysts, the relative rate of alcohol dehydrogenation increased when the inductive effect of the allyl group substituted at the α carbon increased. The same type of relationship was established over the NaY catalysts (Fig. 6). However, it is shown that the slope of the straight line in the latter case is not positive, but equal to zero. There is hardly any difference between the rates of dehydrogenation of the respective alcohols.

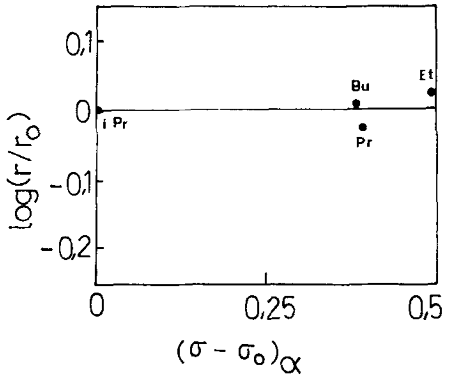

FIG. 6. Variation of the rate of dehydrogenation of different alcohols, over NaY-400 at 120°C, with Taft inductive factors. The reference compound was isopropanol, and the data are for substitution at the α carbon.

DISCUSSION

Nature of the Active Sites

For the high-temperature region, Yashima *et al.* (*2*) advanced the hypothesis that isopropanol was dehydrogenated over basic sites in the zeolite. It was believed that the basicity was related to the $(AlO_4)^-$ tetrahedra paired with alkali cations (*2*).

In this work it is clearly shown that acetone formation at low reaction temperatures does not originate from the dehydrogenation of isopropanol over similar sites. The following evidence clearly shows that residual iron species catalyze the formation of acetone: (i) No relation is observed between the size of the alkali cations and the dehydrogenation activity (Fig. 3); (ii) the influence of reductive and oxidative pretreatments (Table 1) excludes the rate-determining participation of alkali cations; (iii) a direct relation with positive slope is observed between the rate of acetone formation and the residual iron content of the catalysts (Figs. 3, 4); (iv) the amount of acetonitrile poison needed to suppress the dehydrogenation activity is of the same order of magnitude as the residual iron content. The poisoning mechanism has been pictured as due to iron carbide formation (*5*).

Catalyst behavior during dehydrogenation can also be clearly distinguished from its behavior during dehydration: (i) The change of the catalytic activity upon degassing at increasing temperatures is different [for dehydration only one maximum is observed (*4*), while for dehydrogenation two maxima are found (Fig. 1)]; (ii) the influence of the nature of the alkali cation is different. Dehydration activity increases with decreasing size (*4*) of the cation while dehydrogenation does not depend systematically upon the properties of the alkali cation (Fig. 3); (iii) the nature of the major cation (e.g., K^+, Li^+, Na^+, La^{3+}) hardly influences the dehydrogenation, while the introduction of La^{3+} ions results in an increase in the dehydration rate by of least two orders of magnitude (*6*); (iv) the poisoning characteristics for dehydration and dehydrogenation are different. Pyridine poisons the dehydration reaction (*4*), while acetonitrile suppresses the dehydrogenation activity. (Fig. 5).

Mechanism for Dehydrogenation

Kibby and Hall (*2*) conceived the dehydrogenation mechanism of alcohols over hydroxyapatite catalysts to be as follows:

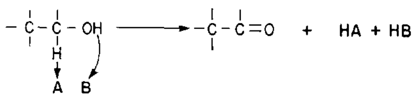

$$-\overset{|}{\underset{|}{C}}-\overset{|}{\underset{\underset{\downarrow}{\underset{H}{|}}}{C}}-OH \longrightarrow -\overset{|}{\underset{|}{C}}-\overset{|}{C}=O + HA + HB$$

An acid–base pair of sites is required for dehydrogenation: The alcoholic proton is discharged to the basic site and the hydrogen atom at the α carbon is discharged to the acid site (*2*). The transition state for this reaction has a high electron density as can be deduced from the positive slope of the linear relation between the logarithm of the relative rates and the Taft inductive factor for substitution at C_α (*2*, *7*, *8*). This is consistent with the rate-determining transfer of a hydride from an adsorbed alkoxide (*2*).

In the zeolite catalysts investigated, the slope of the linear relation between dehydrogenation and Taft inductive factors is close to zero (Fig. 6). This suggests that the rate-determining event is different. On the other hand the observed similarities between the dehydrogenation of isopropanol and the hydrogen–deuterium equilibration suggest that the rate-determining steps might possibly be similar for both reactions. These similarities may be summarized as follows: (i) similar rate changes after treatment of the catalyst in reducing or oxidizing atmospheres; (ii) the same two-maxima activity pattern occurred upon degassing of NaY and LaX and LaY zeolites; (iii) the activation energy remained constant until degassing at 500°C and then gradually declined; (iv) upper numbers of active sites determined with acetonitrile as poison were close together; (v) an identical relation between catalytic activity and residual iron content of the samples was observed.

The H_2–D_2 equilibration reaction was found to occur by a Bonhoeffer–Farkas mechanism, in which the associative desorption of hydrogen determined the rate (*5*). Therefore, the isopropanol dehydrogenation mechanism may be conceived as follows:

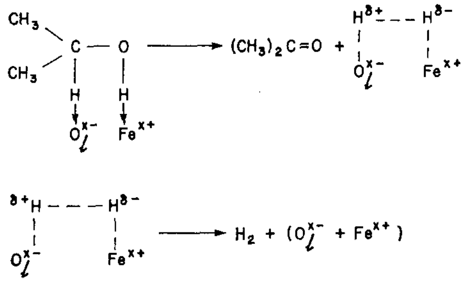

where O_l represents a lattice oxygen and Fe^{x+} an impurity cation. The rate-determining desorption of hydrogen also explains why, in contrast to other solids (*2*, *7*, *8*), a Taft relation with zero slope is obtained.

This detailed mechanism strictly applies only to the first maximum, where iron in cationic positions is proposed to be the active site (*5*). The second maximum in the case of the hydrogen–deuterium exchange is related to the formation of particulate iron oxide, but no detailed mechanism was derived (*5*).

There is one rather important difference between hydrogen equilibration and alcohol dehydrogenation. After activation at 400°C, the former reaction cannot be poisoned completely with acetonitrile (*5*), while this seems possible for the dehydrogenation reaction. The most straightforward explanation is that cationic iron is partly located in the inner cages and partly in the supercages. Both types of sites are available for hydrogen, but not for isopropanol and acetonitrile. The latter two molecules are excluded from the inner sites.

CONCLUSION

Aldehydes or ketones formed over zeolites result from the dehydrogenation of the corresponding alcohols. Cationic iron impurities or particulate iron seems to catalyze the reaction, depending on the activation temperature of the catalysts. The similarities existing between the kinetic data for hydrogen–deuterium equilibration and isopropanol dehydrogenation suggest a reaction mechanism, at least for activation temperatures below 500°C, in which the alcoholic H atom is most probably discharged over cationic iron located in the supercages and the C_α hydrogen atom over a lattice oxygen. As confirmed by a Taft relation, associative hydrogen desorption determines the rate of dehydrogenation.

ACKNOWLEDGMENTS

The skillful experimental help of Mia Tielen is acknowledged. P.A.J. acknowledges a research position as "Bevoegdverklaard Navorser" from the National Science Foundation (N.F.W.O., Belgium). Support from the Belgian Government (Diensten van het Wetenschapsbeleid) is gratefully acknowledged.

REFERENCES

1. Goldstein, R. F., and Waddams, A. L., "The Petroleum Chemicals Industry," p. 339. Spon, London, 1967.
2. Kibby, C. L., and Hall, W. K., *J. Catal.* **29**, 144 (1973).
3. Yashima, T., Suzuki, H., and Hara, N., *J. Catal.* **33**, 486 (1974).
4. Jacobs, P. A., Tielen, M., and Uytterhoeven, J. B., *J. Catal.* **49**, 98 (1977).
5. Heylen, C. F., Jacobs, P. A., and Uytterhoeven, J. B., *J. Catal.* **43**, 99 (1976).
6. Jacobs, P. A., unpublished results.
7. Kraus, M., *in* "Advances in Catalysis" (D. D. Eley, H. Pines, and P. B. Weisz, Eds.), Vol. 17, p. 75. Academic Press, New York, 1967.
8. Van Mechelen, C., and Jungers, J. C., *Bull. Soc. Chim. Belg.* **59**, 597 (1950).